Atomic vibrations in thin [111] $(GaAs)_n(AlAs)_n$ superlattices



1998 J. Phys.: Condens. Matter 10 2829

(http://iopscience.iop.org/0953-8984/10/13/003)

J. Phys.: Condens. Matter **10** (1998) 2829–2843. Printed in the UK PII: S0953-8984(98)90010-8

# Atomic vibrations in thin [111] $(GaAs)_n(AlAs)_n$ superlattices

K Lambert and G P Srivastava

Department of Physics, University of Exeter, Stocker Road, Exeter EX4 4QL, UK

Received 10 December 1997

**Abstract.** We present theoretical investigations of atomic vibrations in thin $(GaAs)_n(AlAs)_n$ superlattices grown in the [111] direction with f.c.c. stacking, using the *adiabatic bond-charge model*. In the acoustic range we confirm the existence of guided Love modes. In the optical range we observe folding, confinement and mode anisotropy behaviours. We show that confined optical modes approximate travelling waves in the propagation layer, decaying rapidly outside. In addition we clearly show optical interface modes of both 'AlAs' and 'GaAs' type, and that these modes are of the 'Fuchs–Kliewer' variety. We compare the results obtained for the [111] direction to previous results obtained for the [001] and [110] directions.

## 1. Introduction

Although semiconductor superlattices (SLs) have been the subject of many investigations recently, these have mainly centred on the electronic and optical properties [1], with fewer studies being carried out on the atomic vibrations. Of these, the majority have been aimed at the $(GaAs)_m(AlAs)_n$ superlattices grown along [001], this being due in the most part to the relative ease of system growth along that direction, and the accompanying experimental data. From Raman scattering measurements [2–8] it has been clearly shown that superlattice formation leads to folded acoustic modes due to the smaller Brillouin zone, confined optical modes caused by boundary discontinuities, and interface modes.

Previous theoretical studies of phonons in semiconductor superlattices have been made by both *ab initio* and phenomenological methods. Superlattice effects on confined phonons were studied by Molinari *et al* [9] using an interplanar force constant method within the pseudopotential approach and local density approximation. Molinari *et al* [10] also used the pseudopotential approach within local density functional linear response theory to investigate phonons in ordered and disordered GaAs/AlAs superlattices. Studies using phenomenological methods have included the application of Rytov's phonon continuum theory by Jusserand *et al* [5] to study folded acoustic modes, the linear chain lattice dynamical model, used by Colvard *et al* [2] to study longitudinal modes, and fully three-dimensional models using the rigid-ion method [11–13] and the bond-charge method [14].

In this work we have used the adiabatic bond-charge model, developed for bulk systems by Weber [15] and Rustagi and Weber [16], to undertake a detailed study of phonon dispersion in $(GaAs)_n(AlAs)_n$ [111] superlattices, where $n/3$ is an integer, and where possible we have compared our results to the [110] and [001] systems [17]. We have examined guided or acoustic interface modes comparing them to the 'Love'- and 'Lamb'-like modes investigated by Richter and Strauch [18], confinement and anisotropy in the optical

0953-8984/98/132829+15$19.50  

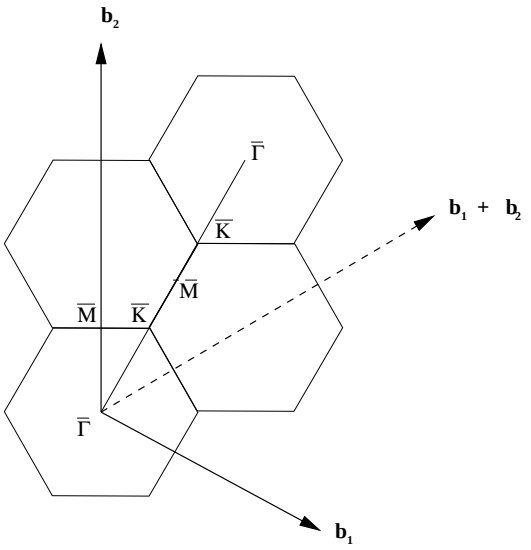


**Figure 1.** A diagram showing the interface Brillouin zone of the cubic [111] superlattices. $b_1$ and $b_2$ indicate the primitive reciprocal-lattice vectors in the interface plane.

range due to boundary discontinuities, together with GaAs-like and AlAs-like interface modes. In addition to agreeing with the theoretical work of Popović *et al* [19] together with the available Raman scattering measurements for the [111] SLs, we have provided new information on AlAs-'like' interface modes. In addition we further the work of Ren *et al* [20] by providing new information on the polarization characteristics of the interface modes.

## 2. Theory

Our method for studying the phonon dispersion in superlattices uses the adiabatic bond-charge model (BCM) developed by Weber [15] for diamond-type structures, and Rustagi and Weber [16], for zinc-blende structures, within a fully three-dimensional periodic approach [17]. The model considers a periodic array of ions, and zero-mass bond charges represent the electronic charge density distributions along the tetrahedral bonds. This three-dimensional periodic approach within the BCM has also been successfully applied in the study of surface phonons on III–V(110) by Tütüncü and Srivastava [21].

The BCM model utilizes three types of interaction: (i) short-range central interactions, (ii) short-range bond-bending interactions, and (iii) long-range interactions due to coulomb forces. The short-range central-force interactions just depend upon the magnitude of the radial distance between the two particles, and the bond-bending interactions considered are of the Keating type [22]. In total, six independent parameters are used in this method, and are taken from the work of Yip and Chang [14].

The phonon eigenvalues and eigenvectors are calculated by solving the secular equation

$$\left|\mathbf{C}_{tot}(\boldsymbol{q}) - \omega^2\mathbf{I}\right| = 0 \tag{1}$$

where $\mathbf{C}_{tot}$ is the total C-type dynamical matrix [23].

Figure 1 shows the interface Brillouin zone for the [111] f.c.c. stacked superlattice. This system is interesting in that all of the symmetry points of the interface Brillouin zone can be

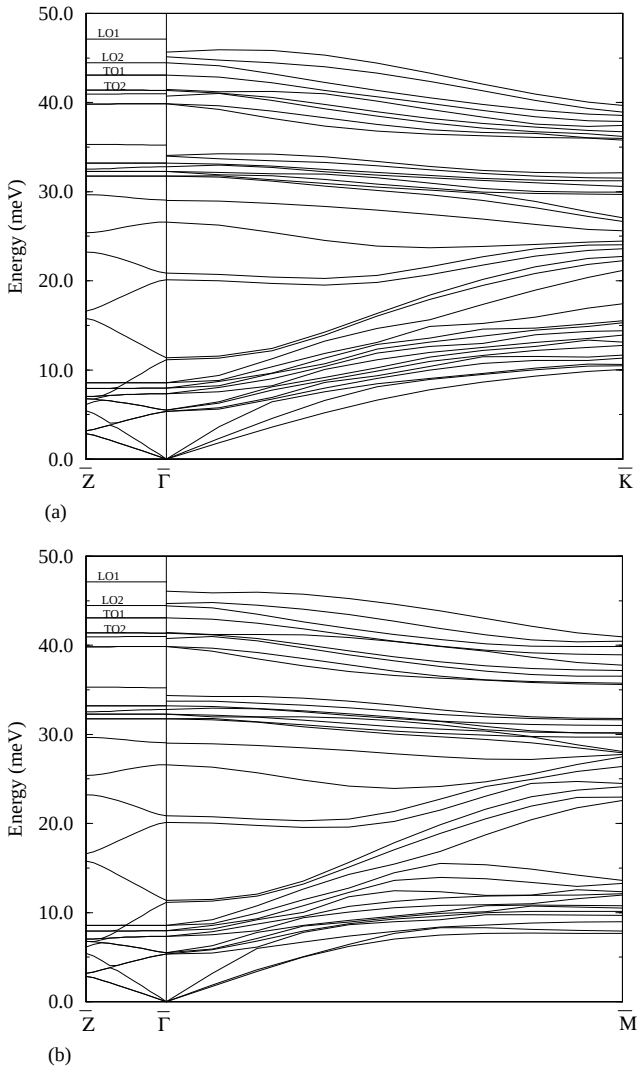


**Figure 2.** Phonon dispersion curves for the $(GaAs)_3(AlAs)_3$ [111] superlattice, displayed in two propagation directions: (a) [111] ($\bar{\Gamma}$–$\bar{Z}$) and [$\bar{1}$01] ($\bar{\Gamma}$–$\bar{K}$) and (b) [111] ($\bar{\Gamma}$–$\bar{Z}$) and [$\bar{1}\bar{1}$2] ($\bar{\Gamma}$–$\bar{M}$).

reached by continued propagation in the [$\bar{1}$01] direction or by encompassing the triangular region shown. The primitive reciprocal-lattice vectors for the [111] interface are given by $\boldsymbol{b}_1 = 2\pi(2/3a)(-1, 2, -1)$ and $\boldsymbol{b}_2 = 2\pi(2/3a)(-1, -1, 2)$, with $a$ equal to the cubic lattice constant.

## 3. Results

We have considered $(GaAs)_n(AlAs)_n$ SLs grown along the [111] direction, with $n$ being a multiple of 3, which we will denote as $(n, n)$ [111]. Detailed studies have been made for optical mode confinement and anisotropy; acoustic mode folding; confinement or guided interface modes; and interface modes in the optical region. Our results are in

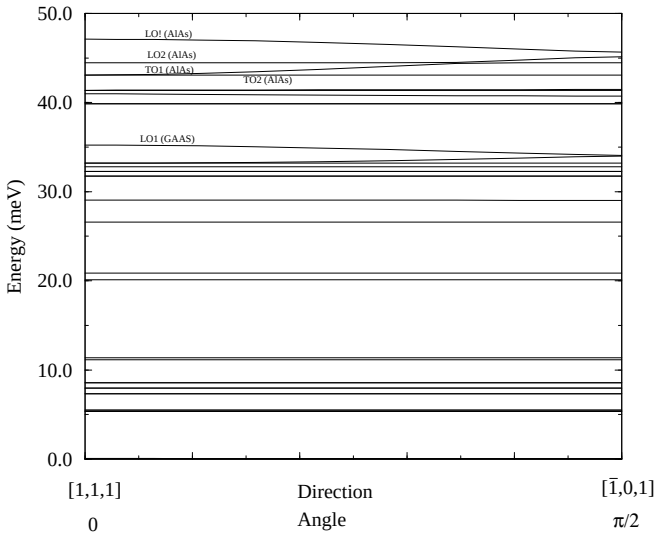


**Figure 3.** The angular variation of optical phonon modes for the $(GaAs)_3(AlAs)_3$ [111] superlattice: phonon energies at a point very close to $\overline{\Gamma}$, with the direction varying from [111] to [$\bar{1}$01] ($\overline{\Gamma}$–$\overline{\mathrm{K}}$).

agreement with the previous studies by Popović *et al* [19] and by Ren *et al* [20]. We have provided information on both GaAs-'type' and AlAs-'type' interface modes, whereas Popović *et al* [19] investigated only GaAs-'type' interface modes and Ren *et al* [20] only provided information on AlAs-'type' modes. We have provided additional information on the polarization characteristics of these AlAs modes, together with a display of primary optic mode frequency as a function of layer width.

### *3.1. Optical mode folding, confinement and anisotropy*

Due to the boundary discontinuities, phonon states in superlattices get confined to the constituent materials. In addition to this well known phenomenon the phonon states also show an angle-dependent anisotropy arising from the macroscopic electric field due to the presence of dipoles at the atomic sites. The total dipole moment inside each slab is approximately proportional to [17, 12]

$$[1-(-1)^n]\cot\frac{n\pi}{2N_s+1}$$

where $N_s$ is the number of bilayers in the material and $n$ is the index of the confined optical mode. This is far more apparent in polar systems such as [001] and [111] systems where bilayers are present, but not so in [110] systems which are essentially non-polar [17, 12].

Figures 2(a) and 2(b) show the difference in the phonon dispersion curves for a (3, 3) [111] superlattice along the growth ($\overline{\Gamma}-\overline{\mathrm{Z}}$) and in-plane ($\overline{\Gamma}-\overline{\mathrm{K}}$ and $\overline{\Gamma}-\overline{\mathrm{M}}$) directions. We can clearly see strong optical mode confinement in the growth direction (the modes labelled LO$n$ and TO$n$ in figure 2), which compare closely to the results obtained for the [001] system [17]. We can also see the anisotropy caused by the non-vanishing dipole moment as we approach the zone centre along the growth and in-plane directions. The primary optic mode LO1 disperses downwards from the growth direction to an in-plane propagation. The magnitudes of this anisotropy are similar for both the ($\overline{\Gamma}-\overline{\mathrm{Z}}$) to ($\overline{\Gamma}-\overline{\mathrm{K}}$) and ($\overline{\Gamma}-\overline{\mathrm{Z}}$) to

($\overline{\Gamma} - \overline{\mathrm{M}}$) direction changes, but a difference is visible nonetheless. Another way of viewing this anisotropy is to take a vanishingly small $\boldsymbol{q}$-vector and vary its propagation direction from 0 to $\pi/2$ radians. Figure 3 utilizes this technique and shows clearly the angular dispersion as the direction is varied from the growth direction to that of $\overline{\Gamma}$ to $\overline{\mathrm{K}}$.

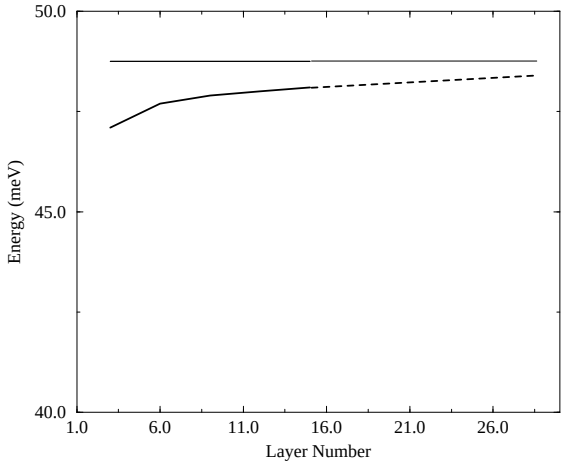


**Figure 4.** A diagram showing the projection of the atomic displacement along the growth direction, as a function of position in the (9, 9) [111] superlattice. The arsenic atoms are denoted by circles, gallium by triangles and aluminium by squares.

Figure 4 shows a graphic example of the degree of confinement experienced by the primary AlAs-'like' optic modes in the $(GaAs)_9(AlAs)_9$ [111] superlattice. The figure depicts (in arbitrary units) the polarization vector of the atom projected along the growth direction as a function of atomic position in the superlattice. The projection is calculated thus [18]:

$$v_z' = \frac{1}{\sqrt{3}}\boldsymbol{v} \cdot [111](-1)^{\kappa}\sqrt{M_{\kappa}} \tag{2}$$

where $\boldsymbol{v}$ is the atomic displacement eigenvector and $M_{\kappa}$ is the atomic mass of the $\kappa$th atom. The factor $(-1)^{\kappa}$ is introduced to take account of the fact that the cations and anions in optic modes vibrate in opposite directions. The figure clearly shows the strong confinement in the aluminium arsenide layers for two optic modes, chosen in this case to be LO1 and LO3 with energies of 47.9 meV and 46.5 meV respectively. We can also see that there is a sinusoidal displacement in the confinement material, together with an exponentially decaying wave in the gallium arsenide layers. This is in agreement with a similar study by Richter and Strauch [18] for the [001] direction.

### *3.2. Confined and guided acoustic modes*

Figure 5 shows the phonon dispersion of the (9, 9) [111] superlattice. The extreme acoustic mode zone folding due to the smaller Brillouin zone is apparent, with the results agreeing closely with the Raman spectra measurements of Popović *et al* [19] for a folded longitudinal acoustic mode at position $\overline{\mathrm{Z}}/5$ and energies of 3.5 and 4.1 meV. In the energy region between 6 and 10 meV (highlighted in figure 5) we can also see confined transverse acoustic modes, with their presence advertised by a flat dispersion in the growth direction. These modes are also known as guided interface modes [18], so called because the interfaces are guiding or

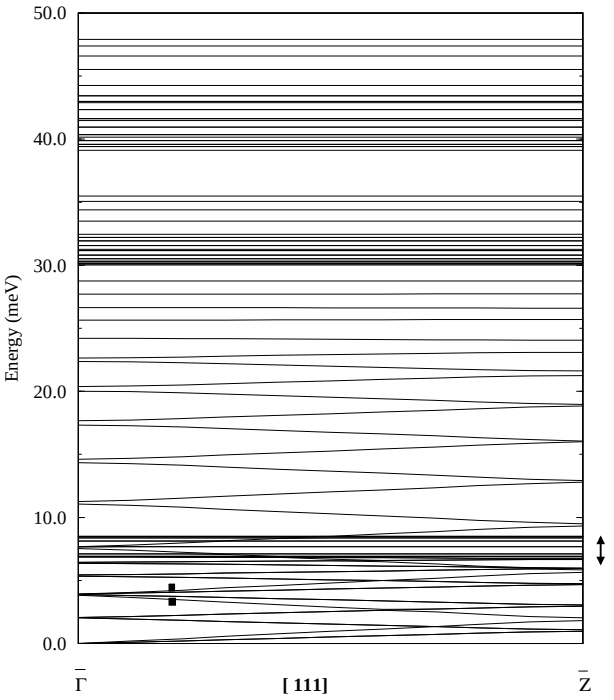


**Figure 5.** A diagram showing the dispersion curves of the $(GaAs)_9(AlAs)_9$ [111] superlattice in the [111] propagation direction. The region of transverse acoustic confined modes is indicated by an arrowed line. Also indicated by closed squares are the folded LA frequencies obtained by Raman measurements [19].

**Table 1.** A table showing the polarization characteristics in the shear horizontal direction $[\bar{1}\bar{1}2]$, and two mutually orthogonal directions in the sagittal plane, the growth direction [111], and $[\bar{1}01]$. Note that at the high-symmetry points $\overline{\Gamma}$ and $\overline{\mathrm{K}}$, mode mixing destroys the pattern.

| Position | Energy (meV) | Displacement (%) $[\bar{1}\bar{1}2]$ | Displacement (%) [111] | Displacement (%) $[\bar{1}01]$ |
|---|---|---|---|---|
| $\overline{\Gamma}$ | 7.22 | 0.0 | 36.6 | 63.4 |
| 0.1 | 7.76 | 1.1 | 0.1 | 98.8 |
| 0.2 | 8.42 | 4.1 | 0.0 | 95.9 |
| 0.3 | 9.36 | 20.7 | 0.0 | 79.3 |
| 0.4 | 10.37 | 15.6 | 0.0 | 84.4 |
| 0.5 | 11.35 | 33.8 | 0.0 | 66.2 |
| 0.6 | 12.24 | 39.3 | 0.0 | 60.7 |
| 0.7 | 12.74 | 50.8 | 0.0 | 49.2 |
| 0.8 | 13.21 | 55.6 | 0.0 | 44.4 |
| 0.9 | 13.84 | 39.9 | 0.0 | 60.1 |
| $\overline{\mathrm{K}}$ | 14.27 | 8.9 | 48.2 | 42.9 |

channelling the modes within a particular material. These modes are not interface modes in the sense that they exist at the interfaces, but more that they are guided by them as a sledge would be channelled down a toboggan run. Having identified these modes by their dispersionless characteristics in the growth direction we can examine them further by

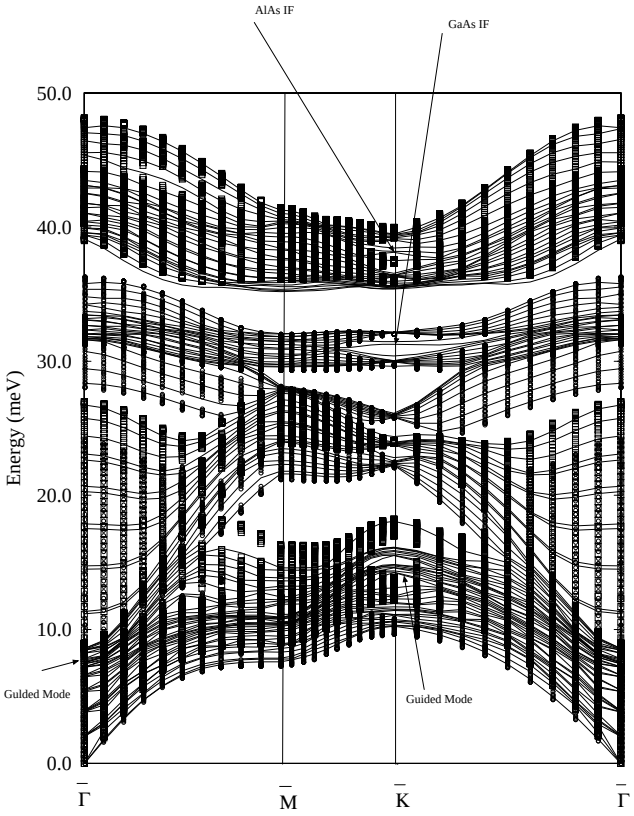


**Figure 6.** Phonon dispersion curves for the $(GaAs)_9(AlAs)_9$ [111] superlattice, shown along the perimeter of the irreducible interface Brillouin zone. The results are overlaid onto the bulk [111] projection in which the AlAs modes are denoted by squares and the GaAs modes by circles. Also indicated are optical interface modes (IF) and guided acoustic modes.

looking at their dispersion and polarizations in in-plane propagations.

Figure 6 shows the dispersion curve for the (9, 9) SL throughout the entire reduced interface Brillouin zone. The dispersion curves are shown overlaying the bulk projections of both gallium arsenide and aluminium arsenide [17]. An interface guided mode is marked at two positions, close to $\overline{\Gamma}$ with an energy of approximately 7.8 meV and close to $\overline{K}$ with an energy of approximately 13.8 meV. This mode near $\overline{\Gamma}$ is shown in figures 7(a) and 7(b) where the projections in the shear horizontal and sagittal planes respectively are shown. Figure 7(a) shows quite clearly that close to $\overline{\Gamma}$ the guided mode is confined quite well to the gallium arsenide layer in the shear horizontal direction. There is almost zero displacement in the sagittal plane as shown by figure 7(b). This is an example of a 'Love' wave, in which the mode displays horizontal displacement transverse to the wave velocity, with exponential decay along the growth direction [18]. Close to $\overline{K}$ the guided mode still shows strong confinement in the GaAs region in the shear horizontal direction and also vibration around the interface in the growth direction. There is still zero displacement in the propagation direction $[\bar{1}0\bar{1}]$. Here the mode is showing characteristics of both 'Love' waves and 'Lamb' waves (which have displacement in the sagittal plane) due to mode mixing away from the zone centre; these displacements are shown in figures 8(a) and 8(b). We have calculated displacements for this mode from the $\overline{\Gamma}$ to $\overline{K}$ points. Table 1 shows the

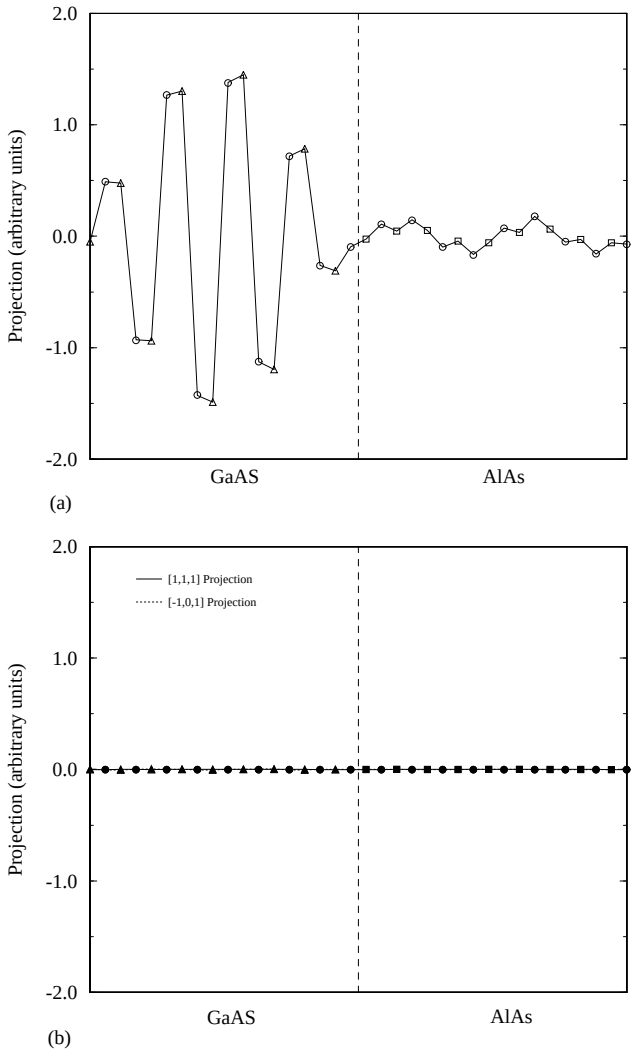


**Figure 7.** The projection of the atomic displacement for a guided acoustic mode near $\overline{\Gamma}$: (a) in the shear horizontal plane and (b) along two mutually perpendicular directions in the sagittal plane. Arsenic atoms represented by circles, gallium atoms by triangles and aluminium atoms by squares.

polarization information as the mode progresses. Neglecting the high-symmetry points, and high degeneracy of $\overline{\Gamma}$ and $\overline{\mathrm{K}}$ we can see that the mode gains a displacement in the growth direction as we approach $\overline{\mathrm{K}}$.

### *3.3. Optical interface modes*

Interface modes are a special feature of superlattices. They propagate in, and are essentially confined to, the interface layers between the two materials, and exist in two forms: (i) macroscopic or electrostatic interface modes due to the electrostatic discontinuities across the interfaces and (ii) microscopic interface modes due to discontinuities caused by large

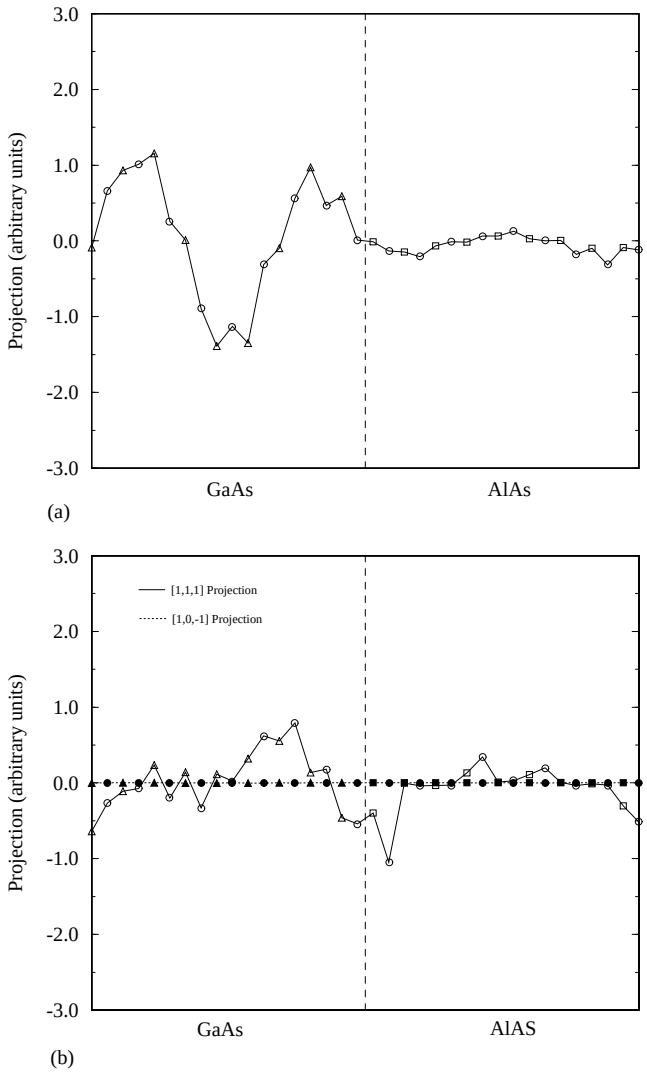


**Figure 8.** The projection of the atomic displacement for a guided acoustic mode at the $\overline{K}$ point: (a) in the shear horizontal plane and (b) along two mutually perpendicular directions in the sagittal plane. Arsenic atoms represented by circles, gallium atoms by triangles and aluminium atoms by squares.

differences in the short-range interactions across the boundaries. As the name suggests, the microscopic interface modes are more highly confined to the interface whilst the macroscopic interface modes tend to penetrate further into the virgin materials [12]. By their very nature, and the fact that they are more likely with superlattice materials of highly differing short-range force constants, these modes are difficult to find in $(GaAs)_n(AlAs)_n$ superlattices where the bond lengths of the materials are very close and the short-range force constants not too dissimilar.

By inspection of figure 6, at the high-symmetry $\overline{K}$ point we can identify two small 'stomach' gaps in the bulk projections, one being in the aluminium arsenide region at approximately 38 meV, and one in the gallium arsenide region at approximately 32 meV.

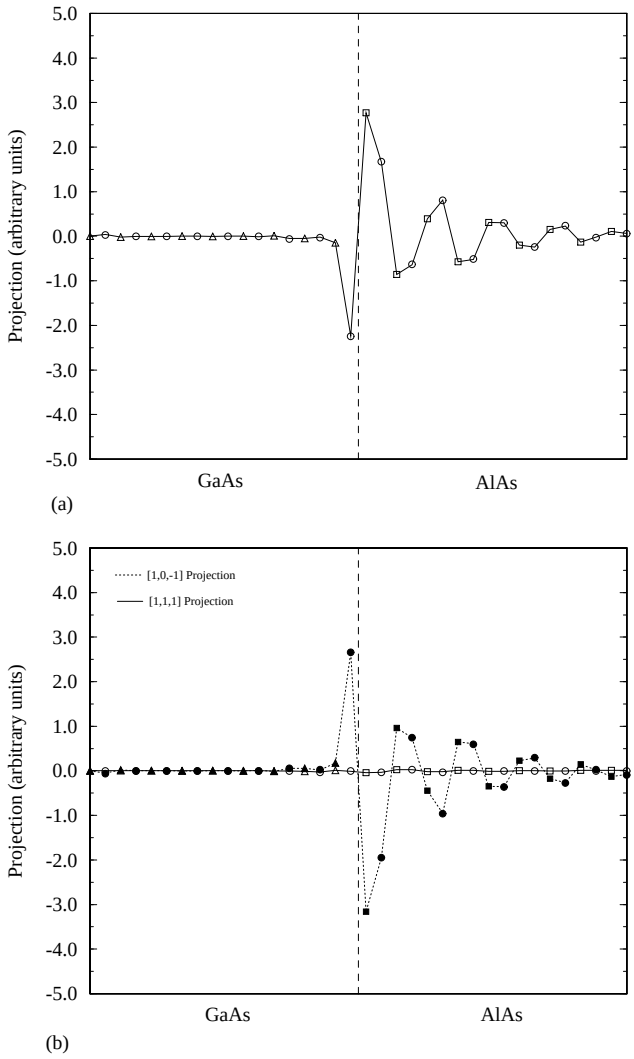


**Figure 9.** The projection of the atomic displacement for an AlAs-'like' optical interface mode of 38.1 meV at the $\overline{K}$ point: (a) in the shear horizontal plane and (b) along two mutually perpendicular directions in the sagittal plane. Arsenic atoms are represented by circles, gallium atoms by triangles and aluminium atoms by squares.

As the gaps indicate frequency ranges denied to bulk phonons, modes that exist in these gaps are likely to be caused by factors pertaining to the superlattice formation, the most obvious feature of which is the interface discontinuities. We have identified two AlAs-like and two GaAs-like interface modes in these pockets.

Figures 9(a) and 9(b) show the polarization information of an aluminium arsenide-'like' mode of energy 38.1 meV at the $\overline{K}$ point mode in both the shear horizontal and the sagittal planes. There is clearly a displacement peak at the GaAs/AlAs interface together with a decaying penetration into the aluminium arsenide slab. There is no noticeable vibration in the gallium arsenide slab. This is characteristic of a macroscopic or 'Fuchs–Kliewer' interface mode [18]. In addition, the vibration in the sagittal and shear horizontal planes

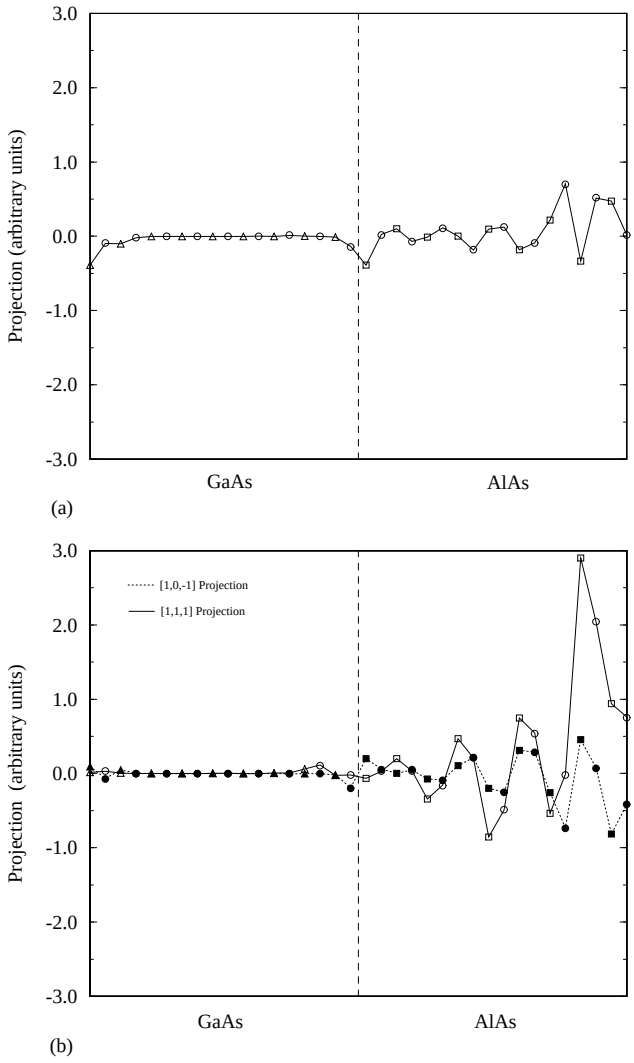


**Figure 10.** The projection of the atomic displacement for an AlAs-'like' optical interface mode of 38.3 meV at the $\overline{K}$ point: (a) in the shear horizontal plane and (b) along two mutually perpendicular directions in the sagittal plane. Arsenic atoms are represented by circles, gallium atoms by triangles and aluminium atoms by squares.

is roughly 50%, with no noticeable vibration parallel to the growth direction as shown by figure 9(b), thus making the displacement totally in-plane.

Figures 10(a) and 10(b) show a macroscopic interface mode at $\overline{K}$ of energy 38.3 meV, again with atomic displacement peaking in the aluminium arsenide region, and with decaying penetration into the AlAs layer. In this case the distribution of vibration in the sagittal and shear horizontal planes is 7:3, and although the vibration still peaks at the interfaces, in this case there is vibration in the direction parallel to the growth direction, in stark difference to the interface mode shown in figure 9.

Figures 11(a) and 11(b) show the atomic displacements of an interface mode in the sagittal plane and shear horizontal direction respectively. The interface mode is in the

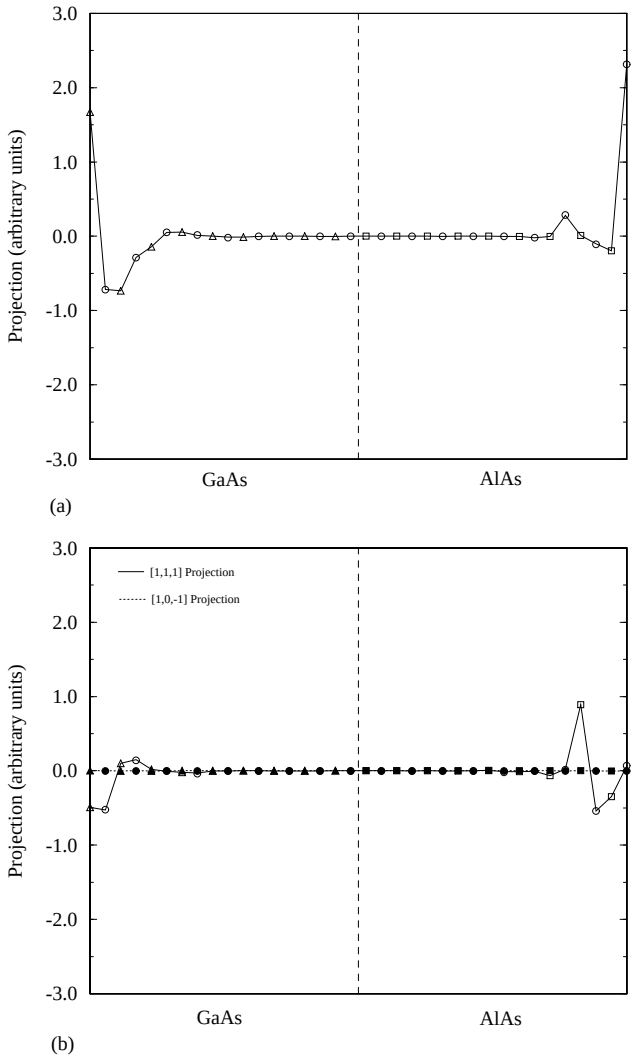


**Figure 11.** The projection of the atomic displacement for an AlAs-'like' optical interface mode of 31.2 meV at the $\overline{\mathrm{K}}$ point: (a) in the shear horizontal plane and (b) along two mutually perpendicular directions in the sagittal plane. Arsenic atoms are represented by circles, gallium atoms by triangles and aluminium atoms by squares.

gallium arsenide region of energy 31.2 meV, with a displacement distribution of 70% in the shear horizontal plane, and 30% in the sagittal plane. The other mode in the stomach gap is a better example, and is shown by figures 12(a) and 12(b). The mode energy is 31.4 meV and again it shows a clear 'Fuchs–Kliewer' characteristic but in this case the vibration distribution between the two planes is evenly split and the mode is better confined to the interfaces.

Optical interface modes are 'Raman active' and comparison with the spectra information in Popović *et al* [19] for these modes gives very good agreement with the Raman peaks shown at approximately 270 to 280 $\mathrm{cm}^{-1}$ (or approximately 33 to 34.5 meV) with our GaAs-like modes at 31.2 and 31.4 meV.

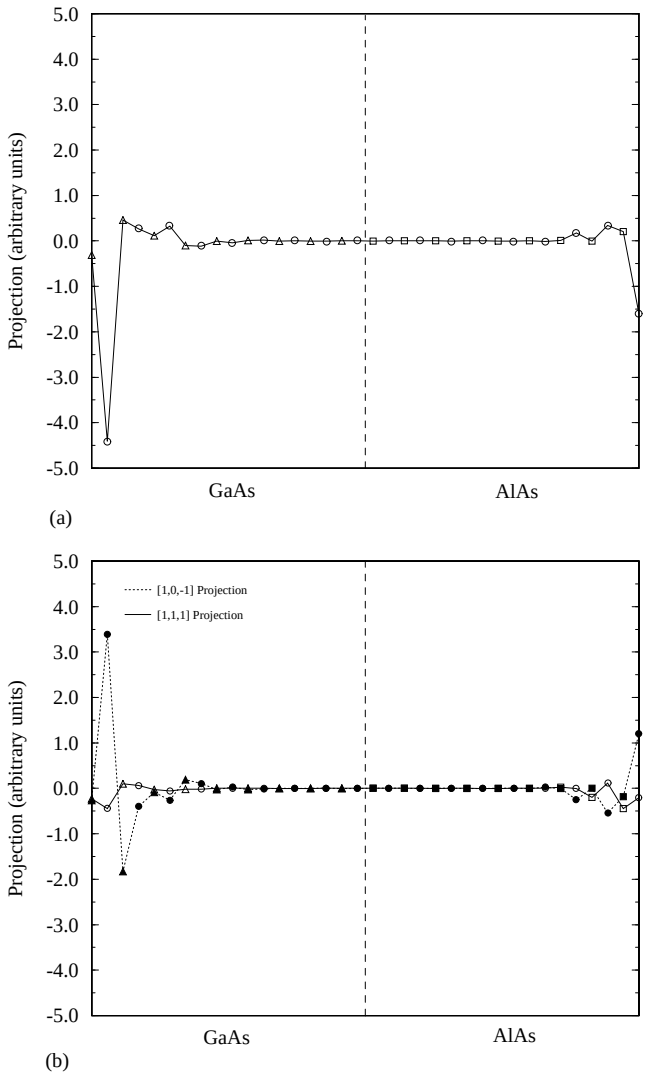


**Figure 12.** The projection of the atomic displacement for an AlAs-'like' optical interface mode of 38.3 meV at the $\overline{K}$ point: (a) in the shear horizontal plane, and (b) along two mutually perpendicular directions in the sagittal plane. Arsenic atoms are represented by circles, gallium atoms by triangles and aluminium atoms by squares.

### *3.4. Mode tendencies with layer width*

As the SL layer thickness increases the highest optical confined mode should progressively move towards the bulk result. In figure 13 we have shown by the unbroken line the dispersion of the AlAs-like LO1 mode as a function of layer thickness. We have extrapolated the result to give some indication of when the primary AlAs-'like' mode attains a bulk value. The figure clearly shows a monotonic variation of the LO mode. A noticeable feature of the [111] SL system is that the LO1 AlAs-like mode does not attain a bulk value for layer thickness index less than 33. A comparable layer index number for the LO1 AlAs-like mode in the [001] system is 15, and 10 for the [110] system [17]. Taking into account the

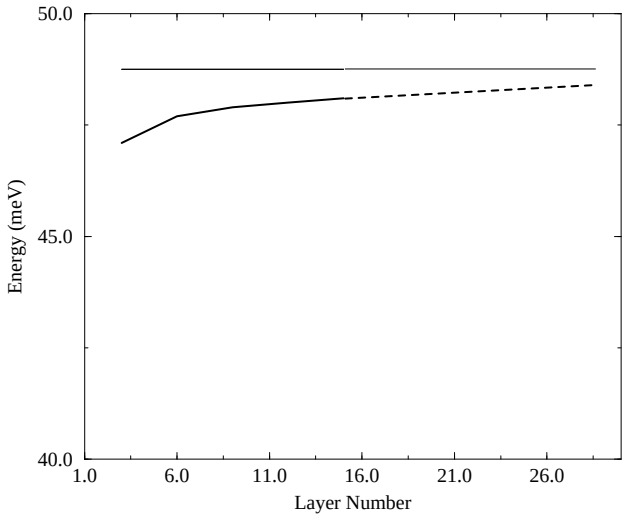


**Figure 13.** A diagram showing the calculated results for the energy of the primary optic AlAs-'like' mode versus layer width in the $(n, n)$ [111] GaAs/AlAs superlattice. The broken line indicates extrapolation of results. The horizontal line refers to the highest LO mode in bulk AlAs.

fact that the width of a layer in the [110] system is $1/\sqrt{2}$ of that of a bilayer in the [001] system, and $\sqrt{3/2}$ of that of a bilayer in the [111] system we can predict that the LO1 AlAs-like modes in the [110] superlattice will reach the bulk value in approximately half the layer width of the [001] case, whilst the AlAs-like modes for the [001] superlattice will reach the bulk value in approximately 0.8 of that of the distance of the [111] case. This is an example of the polarity strength of the system, for, as we have discussed before [17], the [110] SL is essentially non-polar whilst the [001] SL has a dipole moment and bilayers. The [111] SL has an even greater net dipole moment due to its crystal geometry, for, if we take a single arsenic atom as lying at the interface, all three nearest-neighbour cations will lie above (or below) the interface.

## 4. Summary

In this paper we have used the adiabatic bond-charge model, within a three-dimensional periodic approach, to study the phonon dispersion of [111] GaAs/AlAs superlattices. We have confirmed the existence of confined or guided interface 'Love' modes in the acoustic range, shown optical confinement, and optical mode anisotropy. In the case of optical confinement we have also given a detailed polarization picture that shows the sinusoidal characteristics of the modes within the propagating material, together with an exponential decay in the 'forbidden' slab. We have shown detailed polarization data for four optical interface modes in two stomach gaps in the bulk spectra along the reduced interface Brillouin zone, and likened these modes to macroscopic interface modes of the 'Fuchs–Kliewer' type. Two of these GaAs-'type' modes are in good agreement with available Raman data. In addition, we find that the first confined optical mode in the [111] superlattice reaches the bulk-like value in roughly twice the layer width of the [001] system.

## Acknowledgment

KL wishes to express his thanks to the EPSRC (UK) for the award of a studentship.

## References

[1] Cardona M 1990 *Superlatt. Microstruct.* **7** 3
[2] Colvard C, Gant T A, Klein M V, Merlin R, Fischer R, Morkoc H and Gossard A C 1985 *Phys. Rev.* B **31** 4
[3] Jusserand B, Paquet D and Regrenry A 1984 *Phys. Rev.* B **30** 10
[4] Jusserand B, Paquet D, Mollot F, Alexandre F and Le Roux G 1987 *Phys. Rev.* B **35** 6
[5] Jusserand B, Paquet D and Mollot F 1989 *Phys. Rev. Lett.* **63** 21
[6] Jusserand B, Paquet D, Alexandre F and Regrenry A 1986 *Surf. Sci.* **174** 94–7
[7] Sood A K, Menendez J, Cardona M and Ploog K 1985 *Phys. Rev. Lett.* **54** 19
[8] Jusserand B, Alexandre F, Paquet D and Le Roux G 1985 *Appl. Phys. Lett.* **47** 301
[9] Molinari E, Fasolino A and Kunc K 1986 *Superlatt. Microstruct.* **2** 397
[10] Molinari E, Baroni S, Gianozzi P and de Gironcoli S 1990 *Proc. 20th Int. Conf. Physics of Semiconductors (Thessaloniki, 1990)* ed E M Anastassakis and J M Joannopolous (Singapore: World Scientific)
[11] Kanellis G 1986 *Phys. Rev.* B **35** 2
[12] Ren S F, Chu H and Chang Y C 1987 *Phys. Rev.* B **37** 8899
[13] Chu H, Ren S F and Chang Y C 1988 *Phys. Rev.* B **37** 18
[14] Yip S and Chang Y C 1984 *Phys. Rev.* B **30** 12
[15] Weber W 1974 *Phys. Rev. Lett.* **33** 371
[16] Rustagi K C and Weber W 1975 *Solid State Commun.* **18** 673
[17] Lambert K and Srivastava G P 1997 *Phys. Rev.* B **56** 13 387
[18] Richter E and Strauch E 1987 *Solid State Commun.* **64** 867
[19] Popović Z V, Cardona M, Richter E, Strauch D, Tapfer L and Ploog K 1989 *Phys. Rev.* B **41** 5904
[20] Ren S F, Chu H and Chang Y C 1989 *Phys. Rev.* B **40** 3060
[21] Tütüncü H M and Srivastava G P 1996 *J. Phys.: Condens. Matter* **8** 1345
[22] Keating P N 1966 *Phys. Rev.* **145** 637
[23] Maradudin A A 1971 *Theory of Lattice Dynamics in the Harmonic Approximation* 2nd edn (New York: Academic)